J. Iran. Chem. Soc., Vol. 8, No. 3, September 2011, pp. 750-761.

JOURNAL OF THE
Iranian
Chemical Society

All-electron Scalar Relativistic Calculation of the Adsorption of NCO Species onto Small Copper Clusters

X.-J. Kuang[a, b,*], X.-Q. Wang[a,*] and G.-B. Liu[a]

[a]*College of Physics, Chongqing University, Chongqing, 400044, China*

[b]*School of Science, Southwest University of Science and Technology, Mianyang, Sichuan, 621010, China*

(Received 17 July 2010, Accepted 2 December 2010)

An all-electron scalar relativistic calculation of Cu_nNCO (n = 1-13) clusters has been made using density functional theory with the generalized gradient approximation at BLYP level. In all Cu_nNCO clusters, the NCO species prefered to occupy the single-fold coordination site and the small copper cluster tended to bond with the nitric. The Cu_n structures were only distorted slightly and the NCO species retained linear structure. The N-C bond-length contraction and C-O bond-length elongation were observed clearly. The reactivity enhancement of NCO species toward CO_2 was obvious. But, no reactivity enhancement of NCO to form N_2 related to the N-C bond strength could be observed. It seems that the NCO species is more favorably adsorbed by odd-numbered small copper clusters, relatively. Some discrepancies between our work and earlier works were found which may be explained in terms of the scalar relativistic effect. Further studies to focus on the reactivity enhancement of NCO to form N_2 are clearly in order.

Keywords: Small copper cluster, NCO species, Adsorption, All-electron scalar relativistic calculations

INTRODUCTION

The improvement of the catalytic converter technology to decrease automobile exhaust emissions is one of the most important issues of controlling environmental pollution, particularly due to its direct impact on human health. The reduction of air pollution over metal catalysts is of great importance for the removal of pollutant gases from vehicle exhausts. As an isocyanate species, it is known that the NCO is a key intermediate in the rapid reduction of nitrogen oxides process and in the lean NO_x reduction to form N_2 [1-4]. In metal catalysts, NCO is formed on the metal and then migrates on to the support where it can accumulate in considerable amount yielding an intense infrared absorption band due to the asymmetric stretching mode [5]. It is established that the NCO on Cu is more stable than on Pt, Rh and Ru in metal supported catalysts [6-7]. On the latter systems, no NCO is detected above 300 K due to its decomposition or migration to the support. Conversely, it disappears completely on supported Cu catalysts until above 473 K.

Because the involved catalyses reactions primarily occur at infinite surfaces in principle, it makes the theoretical investigations of catalyses difficult. One common solution is to compromise between the solid state physics and molecular physics and use small metal clusters as models for the infinite metal surface. This has been adopted in numerous theoretical investigations of atomic and molecular adsorption onto metallic systems [8-18]. It has been established that some aspects of the adsorbate-substrate interaction, such as the

*Corresponding authors. E-mail: kuangxiangjun@163.com; xqwang@cqu.edu.cn

adsorbate geometries and frequencies are almost cluster size independent. Other aspects, such as the adsorption energies are clearly size dependent. Stimulated by findings of this nature, some theoretical researchers [19-24] have engaged in studying the interaction between NCO species and small copper clusters or Cu surface. Zhao *et al*. have made a density functional calculation for Cu_nNCO^-, Cu_nNCO, Cu_nNCO^+ and Cu_nNCO^{2+} clusters [19]. It was found that for small *n*, charge state had a strong influence on the NCO location site. The ground states of the neutral and anionic complex clusters had a dominantly planar structure while most of the cationic complex clusters prefered three-dimensional structures.

The electrostatic interaction was essential for the Cu-NCO bond, while covalent interaction through 2π donation strongly enhanced the bond. In neutral and anionic species, the N-C bonds were strengthened and the C-O bonds were weakened, while in cationic species all the C-O distances decreased and the N-C distances were slightly elongated in some cases, which is related to a higher NCO reactivity toward NO and O_2 to form N_2 over the positively charged $Cu_n^{\delta+}$ sites than that over the metallic Cu_n sites. The adsorption of cyanato radial (OCN) on Cu (100) surface was studied by using density functional theory (DFT) and the cluster model method. Cu_{14} cluster was used to simulate the surface [20]. Our calculations showed that cyanato-N species, absorbed on the surface, was more favorable than on other configurations. NCO species was linearly bonded to the Cu (100) surface via the nitrogen atom. The calculated symmetric and asymmetric OCN stretch frequencies were all blue-shifted compared with the calculated gaseous values. The charge transfer from the surface to OCN caused a work function increase on the surface. The bonding of OCN to the metal surface was largely ionic.

Although there are some theoretical research reports on the adsorption behavior of NCO species onto bare Cu_n (n = 1-6) clusters [19], cluster size up to six is far from enough further investigation on the adsorption behavior of some large copper clusters is in order. Furthermore, previous studies [25] have indicated that as a heavy coinage metal element, the scalar relativistic effect of the outer shell electrons in gold clusters is obvious and may cause a shrinking of the size of *s* orbitals and thus enhance the *s-d* hybridization. This is most strikingly evident in the gold clusters and is called “gold maximum” [26]. Due to the similar atomic configuration, it is reasonable to assume that the influence of scalar relativistic effect on the adsorption behavior of small silver and copper clusters might also exist. Thus, it is necessary to include the scalar relativistic effect in the study of NCO species onto small copper clusters.

In this paper, we shall do an all-electron scalar relativistic (AER) calculation on the NCO species adsorption onto small copper clusters (n = 1-13) by using the density functional theory with the generalized gradient approximation at BLYP level. The goal of this work is to gain a deep and comprehensive understanding of the interaction between NCO species and small Cu_n (n = 1-13) clusters as a first step for understanding the role Cu clusters play in the formation of N_2 and CO_2 from NCO. It is also of great significance to investigate the influence of the scalar relativistic effect on the adsorption behavior of NCO species onto small copper clusters by making a close comparison with the previous works without including the scalar relativistic effect [19]. The paper is arranged as follows: the computational method and cluster model are described in Section 2, calculation results and discussions are presented in Section 3 and the main conclusions are summarized in Section 4.

COMPUTATIONAL METHOD AND CLUSTER MODEL

The geometrical structures and electronic properties of Cu_nNCO (n = 1-13) clusters were calculated by using the density functional theory (DFT). Under the framework of DFT, the scalar relativistic effect was included for the reason described in Section 1. The numerical atomic orbitals were used in the construction of the molecular orbitals. In many previous cases, as an approximation, only the outer shell atom-orbitals were employed to generate the valence orbitals and the rest of the core orbitals were frozen. Although the calculations involving all-electron scalar relativistic (AER) method were rather difficult to make due to the high computational expenses, they were supposed to provide a better accuracy than those only involving all-electron (AE) and effective core potentials (ECP). The advantages of the all-electron scalar relativistic (AER) method over the effective core potential (ECP) method and all-electrons (AE) method have been demonstrated by some researchers [27-29]. Considering the above factors and in order to improve the

calculation accuracy, we did an all-electron scalar relativistic (AER) calculation and used the corresponding high quality DNP basis set despite the vast computational expense.

The PW91 and BLYP forms of GGA for the exchange-correlation functional were adopted in the calculations on bare Cu_n clusters and Cu_nNCO clusters, respectively. The SCF tolerance was set to be 1.0×10^{-6} eV. In order to accelerate the calculation, the direct inversion in iterative subspace (DIIS) approach was used and the smearing value was set to be 0.005*Ha*. During the structure optimization, the spin was unrestricted and the symmetry of the structure had no constraint. The convergence tolerance of max force, max energy and max displacement was 0.002 *Ha*/*Å*, 1.0×10^{-5} *Ha* and 0.005 *Å*, respectively.

During the structure relaxation, the spin multiplicity was considered to be at least 2, 4 and 6 for odd-electron Cu_nNCO clusters (n = 2, 4, 6, 8, 10 and 12) and 1, 3, 5 for even-electron Cu_nNCO clusters (n = 1, 3, 5, 7, 9, 11 and 13). When the total energy decreased with the increasing of spin multiplicity, the high spin state was considered until the energy minimum with respect to the spin multiplicity was reached. In addition, the stability of the optimized geometry was confirmed without any imaginary frequency by computing vibrational frequencies at the same level of theory. All these calculations were made by using the Accelrys Dmol 3.0.1 program package [30-31].

The choice of distinct initial geometries was important to obtain the lowest energy structures. In this work, we got the initial structures in the following way. First, considering the previous studies on the configurations of pure copper clusters [32-40], we optimized the structures of pure Cu_n (n = 2-13) cluster by using the same method and same parameters. On the basis of the optimized equilibrium geometries of pure cooper clusters, we obtained the initial structures of Cu_nNCO clusters by approaching NCO species directly on each possible nonequivalent site of Cu_n cluster, including all possible bonding patterns. All these initial structures were fully optimized by relaxing the atomic positions until the force acting on each atom vanished (typically $|F_i| \leq 0.002$*Ha*/*Å*) and by minimizing the total energy.

In order to check the intrinsic reliability of various functional forms, we chose Cu_3, Cu_4, NCO and Cu_2NCO as examples to calculate some properties (the corresponding experimental data are available for these clusters) by using the GGA-PW91, GGA-BP, GGA-PBE, GGA-BLYP and LDA-PWC, LDA-VWN functional forms, respectively. From the calculation results listed in Table 1, we can see that for Cu_3 and Cu_4 clusters, the results obtained by using the GGA-PW91 functional form are closer to the available experimental data [32-40]. But, for free NCO species and Cu_2NCO cluster, the results obtained by using the GGA-BLYP functional form are closer to the available experimental data [41-45]. This indicates that among all these available functional forms, the GGA-PW91 is the most reliable and accurate one for the study of pure Cu_n clusters and the GGA-BLYP is the most reliable and accurate one for the study of free NCO species and Cu_nNCO clusters.

Table 1. Results Comparison between Different Functional Forms for Some Properties of Cu_3, Cu_4, NCO and Cu_2NCO Clusters

Cluster	Cu_3	Cu_4	NCO		Cu_2NCO
properties	E_b (eV atom^{-1})	E_b (eV atom^{-1})	$R_{N\text{-}C\text{-}O}$ (Å)	$\nu_{N\text{-}C\text{-}O}$ (cm^{-1})	$\nu_{N\text{-}C\text{-}O}$ (cm^{-1})
GGA-PW91	1.189	1.580	2.426	1993.3	2222.7
GGA-BP	1.114	1.434	2.430	1985.9	2217.6
GGA-PBE	1.200	1.533	2.429	2012.6	2212.4
GGA-BLYP	1.117	1.410	2.412	1921.0	2176.8
LDA-PWC	1.558	1.956	2.422	2029.3	2279.4
LDA-VWN	1.553	1.952	2.420	2030.3	2280.5
Experiment data	1.190	1.620	2.406	1921.3	2165.0

RESULTS AND DISCUSSION

Geometrical Structures

In order to obtain the initial structures of Cu_nNCO clusters, the fully optimized structures of bare Cu_n clusters are depicted in Fig. 1. These structures are in good agreement with the available previous works [32-40]. Based on the optimized lowest energy structures of bare copper clusters, we carried out an extensive lowest energy structures research on NCO species adsorption onto small copper clusters by using the GGA-BLYP functional form as was described in Section 2. The fully optimized geometries of Cu_nNCO (n = 1-13) clusters including some low-lying geometric isomers with higher energy and the free NCO species are depicted in Fig. 1. From

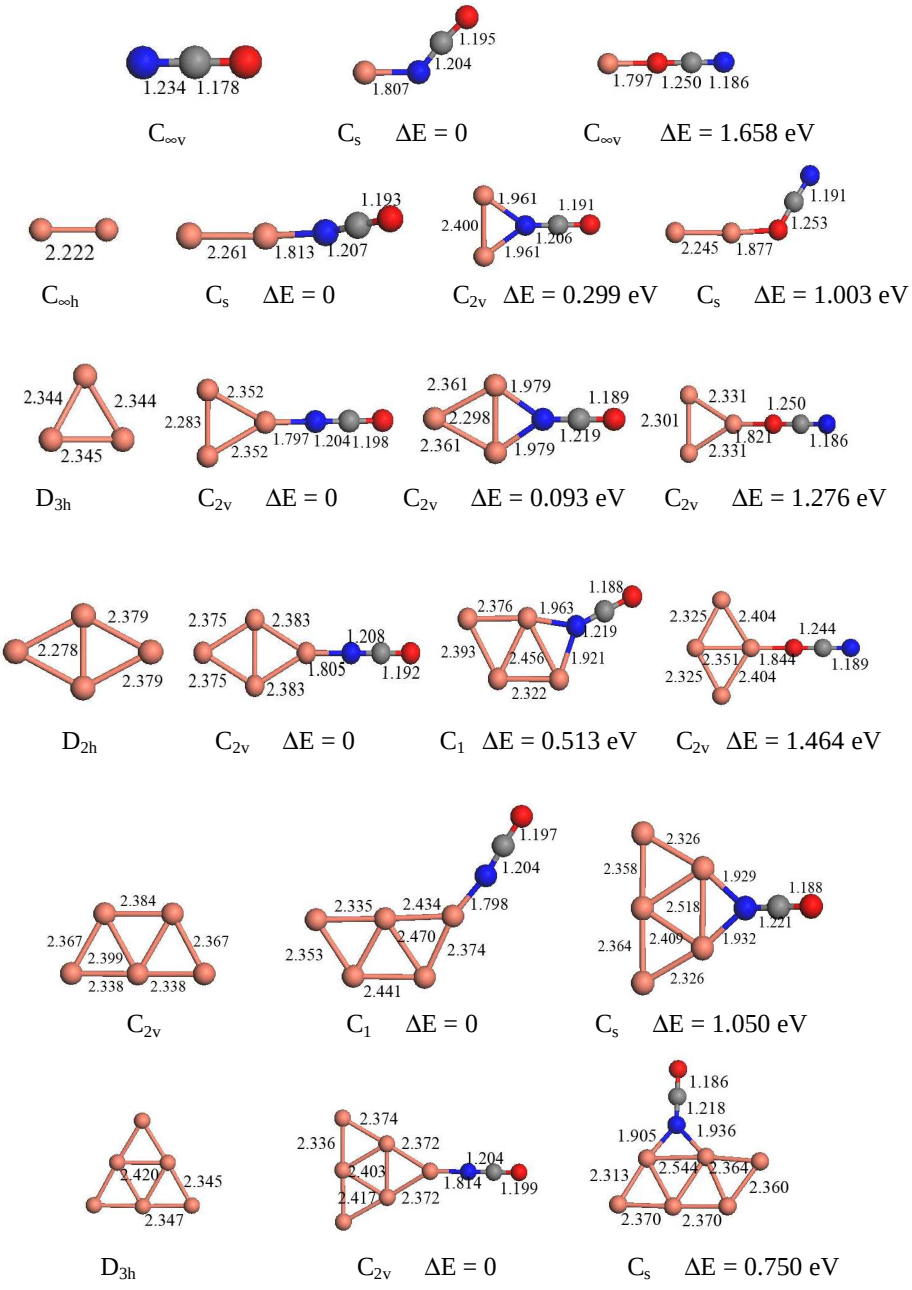

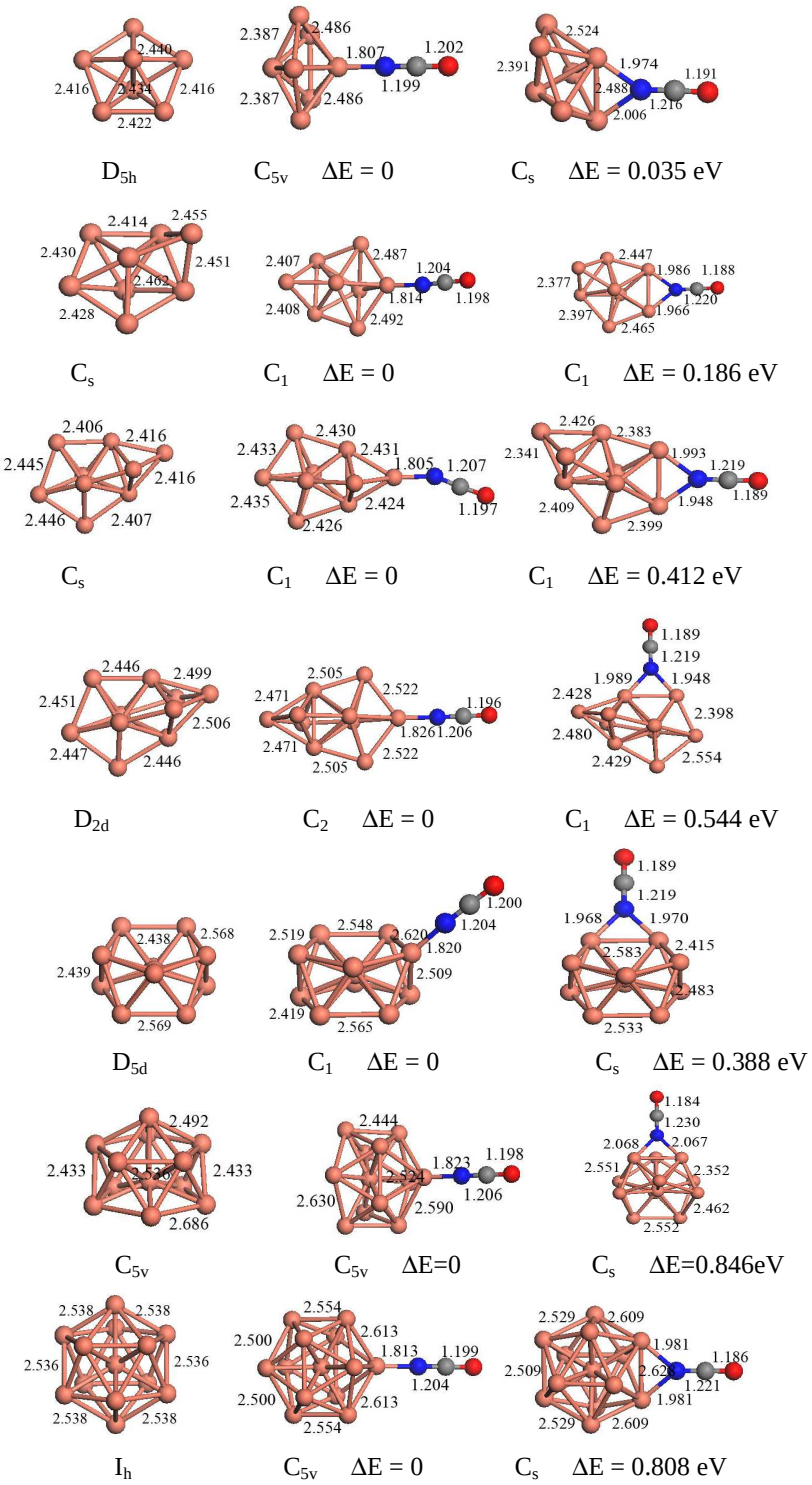

Fig. 1. Optimized geometries for pure Cu_n (n = 2-13) clusters, free NCO species and Cu_nNCO (n = 1-13) clusters. The average Cu-Cu, Cu-N, N-C and C-O bond lengths in angstrom are shown next to each cluster.

these figures, we can find that for all Cu_nNCO (n = 1-13) clusters, the NCO species prefers to occupy the single-fold coordination site for the lowest energy geometries and the two-fold coordination bridge site for the low-lying geometric isomers with higher energy. This picture is obviously different from the previous work [19], in which the NCO species prefers to occupy the two-fold coordination bridge site for the lowest energy geometries of Cu_nNCO (n = 1-6) clusters.

The small copper clusters tended to bond with nitric rather than with carbon and oxygen or with both two and three atoms of NCO species. Compared with the structures of bare Cu_n clusters and free NCO species, the Cu_n structures in all Cu_nNCO clusters were only distorted slightly, the NCO species was also slightly perturbed and retained linear structure without bent. After adsorption, most of the Cu-Cu bond-lengths became longer and only a few Cu-Cu bond-lengths far from NCO species became shorter in Cu_nNCO clusters with the exception of the Cu_2NCO cluster. Similar to the previous work [19], the N-C bond-length became shorter and the C-O bond-length became longer. It is inferred that after adsorption, the N-C bond was strengthened, while the C-O bond and most of the Cu-Cu bonds were weakened. The reactivity of NCO to form CO_2 related to the C-O bond strength was obviously enhanced.

Unfortunately, we did not find any reactivity enhancement of NCO to form N_2 related to the N-C bond strength. This could be explained in terms of the electron donation from the 2π orbital of NCO to the $d\sigma$+sp hybridized orbital of Cu and the electron back donation from the occupied $d\pi$ orbital of Cu to the unoccupied 2π orbital of NCO species [46], which resulted in the strengthening of Cu_n-NCO bond, and N-C bond and the weakening of C-O bond. This is comparable to the previous study on the NCO species adsorption on Cu surface [21-22]. Moreover, the Cu-N bond-length in odd-numbered Cu_nNCO cluster is shorter than that in the adjacent even-numbered Cu_nNCO cluster. The Cu-N bond-lengths of Cu_nNCO clusters exhibit an obvious odd-even oscillation (see Fig. 1), indicating that the Cu-N bond in the odd-numbered Cu_nNCO cluster is stronger than that in the adjacent even-numbered Cu_nNCO cluster, relatively.

Energy and Electronic Structure

The adsorption energies E_{ad}, HOMO and LUMO energy levels, HOMO-LUMO gaps (HLG), Fermi energy levels, vertical ionization potentials (VIP) for Cu_nNCO (n = 1-13) clusters are listed in Table 2, where we define: $E_{ad} = [E(Cu_n) + E(NCO) - E(Cu_nNCO)]$ and $VIP = E(Cu_nNCO)^+ - E(Cu_nNCO)$, respectively. From the adsorption energies displayed in Table 2, we can see that by increasing the number of copper atoms, the adsorption energy of odd-numbered Cu_nNCO cluster became larger than that of the adjacent even-numbered Cu_nNCO cluster. The odd-even oscillation of adsorption energies in Cu_nNCO clusters was obvious. It is suggested that the adsorption strength between NCO species and odd-numbered copper cluster was stronger than the adsorption strength between NCO species and even-numbered copper cluster. It seems that the NCO species was more favorably adsorbed by odd-numbered small copper clusters, relatively. This is similar to the previous work where it was explained in terms of the electron pairing effect [19].

The vertical ionization potential (VIP) is often used to investigate the chemical stability of small clusters, the larger VIP, the deeper HOMO energy level, which leads to less reactivity or higher chemical stability. HOMO-LUMO gap (HLG) is another useful parameter for examining the electronic stability of a cluster. A larger HLG requires higher energy to excite the electrons from valence band to conduction band, corresponding to the higher stability of electronic structure. From the data listed in Table 2, we can find that the VIP and HLG of odd-numbered Cu_nNCO cluster are larger than those of the adjacent even-numbered Cu_nNCO cluster. Furthermore, the HOMO (LUMO) energy level and Fermi energy level of odd-numbered Cu_nNCO cluster are higher than those of the adjacent even-numbered Cu_nNCO cluster. The VIPs, HLGs, HOMO (LUMO) energy levels and Fermi energy levels of Cu_nNCO clusters have obvious odd-even oscillation. It is believed that the odd-numbered Cu_nNCO cluster might be more stable than the adjacent even-numbered Cu_nNCO cluster electronically and chemically. This odd-even oscillation can also be observed in H binding onto small gold clusters and explained in terms of the electron pairing effect [9].

For a cluster, the number of electrons in the HOMO determines its ground-state electronic configuration. By the orbital occupation analysis, we can find that the HOMOs of odd-numbered Cu_nNCO clusters with even number of valence electrons are fully occupied by the majority spin and minority

Table 2. Some Calculated Results of Geometry and Energy Structure for Cu_nNCO (n = 1-13) Clusters

Cluster	$\Delta R_{N-C}/R_{N-C}$ percentage	$\Delta R_{C-O}/R_{C-O}$ percentage	E_{ad} (eV)	HOMO (eV)	LUMO (eV)	HLG (eV)	E_F (eV)	VIP (eV)
CuNCO	2.431%	1.443%	3.519	-5.756	-4.133	1.623	-5.079	9.199
Cu_2NCO	2.188%	1.273%	2.601	-4.714	-4.234	0.480	-4.413	7.213
Cu_3NCO	2.431%	1.698%	4.215	-5.471	-4.035	1.436	-4.756	8.034
Cu_4NCO	2.107%	1.188%	3.560	-4.711	-4.160	0.551	-4.175	7.104
Cu_5NCO	2.431%	1.613%	4.402	-5.391	-3.978	1.413	-4.344	7.579
Cu_6NCO	2.431%	1.783%	3.495	-4.635	-4.191	0.444	-4.255	6.621
Cu_7NCO	2.836%	2.037%	4.355	-5.127	-3.936	1.191	-4.321	7.197
Cu_8NCO	2.431%	1.698%	3.451	-4.513	-4.079	0.434	-4.235	6.599
Cu_9NCO	2.188%	1.613%	3.905	-4.802	-3.564	1.238	-3.933	7.451
$Cu_{10}NCO$	2.269%	1.528%	3.471	-4.213	-3.973	0.240	-4.075	6.240
$Cu_{11}NCO$	2.431%	1.868%	3.922	-5.097	-3.890	1.207	-3.991	7.129
$Cu_{12}NCO$	2.269%	1.698%	3.525	-4.401	-4.011	0.390	-4.121	5.911
$Cu_{13}NCO$	2.431%	1.783%	3.914	-5.115	-3.865	1.250	-3.974	7.208

Table 3. The Charge Transfer, Electronic Configuration, Spin Multiplicity (M) and Magnetic Moment for Cu_nNCO Clusters

Cluster	Charge				Electronic configuration	M	Magnetic moment (μ_B)		
	NCO	N	C	O			Cu_n	NCO	Total
CuNCO	-0.983	-1.117	0.753	-0.619	closed	1	0	0	0
Cu_2NCO	-0.957	-1.103	0.742	-0.596	open	2	0.917	0.083	1
Cu_3NCO	-1.003	-1.115	0.745	-0.633	closed	1	0	0	0
Cu_4NCO	-0.975	-1.121	0.758	-0.612	open	2	0.922	0.078	1
Cu_5NCO	-1.016	-1.124	0.747	-0.639	closed	1	0	0	0
Cu_6NCO	-0.931	-1.107	0.801	-0.625	open	2	0.899	0.101	1
Cu_7NCO	-1.010	-1.128	0.764	-0.646	closed	1	0	0	0
Cu_8NCO	-0.929	-1.100	0.791	-0.620	open	2	0.941	0.059	1
Cu_9NCO	-1.018	-1.118	0.749	-0.649	closed	1	0	0	0
$Cu_{10}NCO$	-0.983	-1.107	0.755	-0.631	open	2	0.980	0.020	1
$Cu_{11}NCO$	-1.029	-1.119	0.744	-0.654	closed	1	0	0	0
$Cu_{12}NCO$	-0.960	-1.104	0.803	-0.659	open	2	0.967	0.033	1
$Cu_{13}NCO$	-1.023	-1.122	0.752	-0.653	closed	1	0	0	0

spin electrons, which leads to ground state of these clusters with closed electronic shells and are stable remarkably. But, the HOMOs of even-numbered Cu_nNCO clusters with odd number of valence electrons are occupied partially only by majority spin electrons and have open electronic shells (see Table 3). According to the Jahn-Teller theorem, these clusters have the tendency to distort further toward lower symmetry in order to reduce or remove their degeneracies and lower their

energies. However, we must point out that the open shell cluster may also increase its degeneracy and have high spin multiplicity if it possesses a decreased total energy. It depends on a compromise between the decreasing of total energy and the increasing of degeneracy. This compromise will decide whether or to what extent the Jahn-Teller distortion may take place [47-48].

The interaction between copper cluster and NCO species can also be reflected through charge transfer. We performed a Mulliken charge analysis for Cu_nNCO clusters and listed the effective charges on N, C, O and NCO in Table 3. The values of charge transfer suggest a mechanism in favor of back-donation, that is, charge transfer from the copper cluster to the NCO species, the NCO species behaves as a charge acceptor. As a result of this charge transfer, both the N-C bonding orbital and C-O anti-bonding orbital were filled with more electrons, leading to the stabilization of N-C bond and the destabilization of C-O bond, appearing as the shortening of N-C bond-length and the lengthening C-O bond-length, which can be observed clearly in Fig. 1. A similar behavior of bond-length variation related to the charge transfers from Cu to NCO species has been reported in the previous study on the NCO adsorption on Cu surface [21-22]. Apparently, the greater charge transfer often leads to larger adsorption energy and this can be confirmed by the NCO species adsorption onto small copper clusters. The charge transfer in odd-numbered Cu_nNCO cluster with larger adsorption energy is greater than that in even-numbered Cu_nNCO cluster with smaller adsorption energy. The charge transfer of Cu_nNCO clusters also shows an obvious odd-even oscillation. This is similar to the NO adsorption onto small gold clusters [46] and proves again that the NCO species is more favorably adsorbed by the odd-numbered Cu_n clusters.

In order to understand the nature of chemical bonding in these systems, we have plotted the spatial orientations of HOMO for Cu_nNCO clusters and NCO species in Fig. 2. At first glance, the HOMOs of these clusters are delocalized obviously with a contribution from almost all atoms in the cluster. The strong *sd* orbital hybridization between copper atoms and the *sp* orbital hybridization in NCO are very

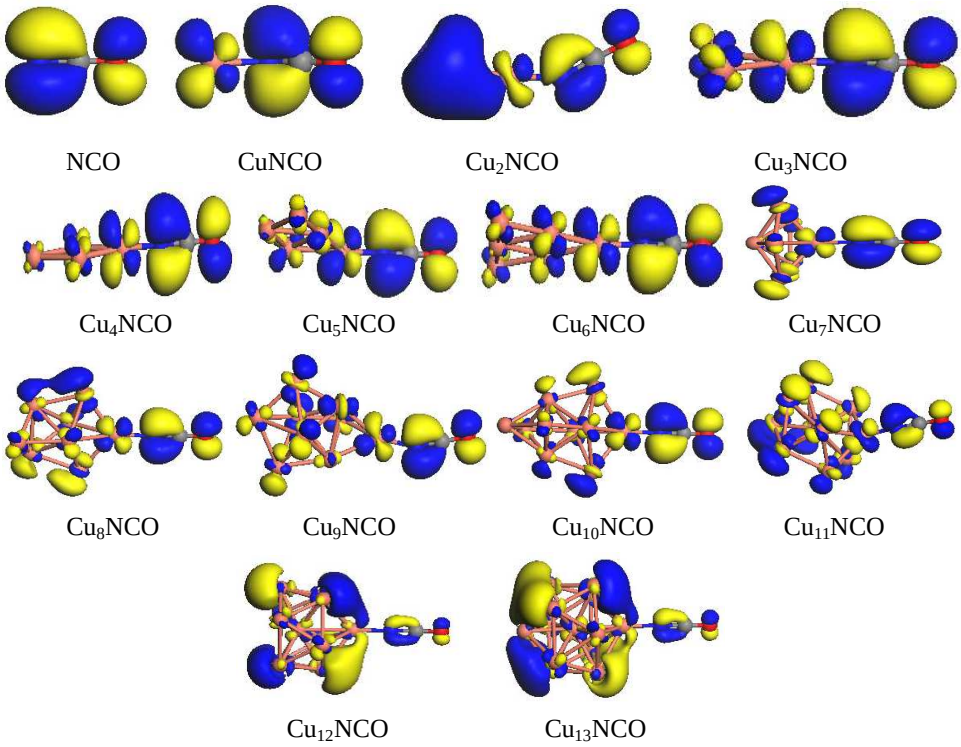

Fig. 2. The spatial orientations of HOMO for Cu_nNCO (n = 1-13) clusters and free NCO species.

obvious. The HOMO shapes of NCO in all Cu_nNCO clusters are similar to the HOMO shape of free NCO species which has a $^2\Pi$ ($7\sigma^2 2\pi^3$) frontier molecular orbital. All these 2π molecular orbitals are characterized by a bonding orbital between N and C and an anti-bonding orbital between C and O. The covalent interaction between Cu_n cluster and NCO species can be implemented mainly through the electron back donation from the occupied $d\pi$ orbital of Cu_n to the unoccupied 2π orbital of NCO species, the electron donation from the 2π orbital of NCO to the $d\sigma$+*s* hybridized orbital of Cu_n and the electrostatic interaction between metal ions and the lone pair of the N atom.

Frequency Analysis

Since many experiments on the adsorption behavior of nanosized transitional metal clusters are based on the FTIR method and focus on the vibrational frequency of different modes in the adsorption system, in Table 4, we give the highest frequencies of Cu-Cu, Cu-N, N-C-O mode for Cu_nNO clusters and Cu-Cu, N-C-O mode for pure Cu_n clusters and free NCO species, respectively. It is easy to notice that the highest vibrational frequency of Cu-N mode for odd-numbered Cu_nNCO cluster is obviously higher than that of Cu-N mode for even-numbered Cu_nNCO cluster. Likewise, an obvious odd-even oscillation can be observed. This frequency variation is approximately parallel to the variations of Cu-N bond-lengths, adsorption energies, charge transfers, VIPs, HLGs, HOMO (LUMO) energy levels, Fermi energy levels and confirms again that the Cu-N bond in odd-numbered Cu_nNCO cluster is relatively stronger than that in the adjacent even-numbered Cu_nNCO cluster.

Due to the strengthening of N-C bond, the highest vibrational frequencies of N-C-O mode for all Cu_nNCO clusters are higher than the highest vibrational frequency of N-C-O mode for free NCO species. With the exception of Cu_2NCO cluster, the highest vibrational frequency of Cu-Cu mode in Cu_nNCO (n = 3-13) cluster is slightly higher than that of Cu-Cu mode in the corresponding pure Cu_n cluster. This is entirely consistent with the strengthening of the Cu-Cu bonds which are far from NCO species in Cu_nNCO clusters.

Magnetic Properties

Finally, we will discuss the magnetic properties of Cu_nNCO clusters. From Table 4, we can see that all the Cu_nNCO clusters prefer low spin multiplicity (M = 1 for odd-numbered Cu_nNCO clusters and M = 2 for even -numbered Cu_nNCO clusters). The odd-numbered Cu_nNCO clusters were found to exhibit zero magnetic moment and the even-numbered Cu_nNCO clusters were found to possess magnetic moment with the value of 1 μ_B (mainly contributed by Cu_n). This odd-even alteration of magnetic moments for Cu_nNCO clusters is quite obvious and may serve as the material with tunable code capacity of “0” and “1” [49], and can also be simply understood by considering the electron pairing effect. Based on the valence electron configuration of $Cu4s^1$, $N2s^22p^3$, $C2s^22p^2$ and $O2s^22p^4$, respectively, as NCO species is adsorbed onto odd-numbered Cu_n cluster, the odd number of 4s electrons from copper cluster and the odd number of 2s and 2p electrons from NCO species tend to form a closed electronic structure according to the Hund’s rule, so the odd-numbered Cu_nNCO clusters show zero magnetic moment according to Pauli repulsion in the case of the electron pairing.

As NCO species is adsorbed onto even-numbered Cu_n cluster, the even number of 4s electrons from Cu cluster and the odd number of 2s and 2p electrons from NCO species prefer to form an open electronic structure according to the Hund’s rule and possess the magnetic moment of $1\mu_B$ with one unpaired electron. Some studies [50-52] have shown that charge transfer and hybridization of valence electrons stemming from host and impurity influence the local magnetic moment significantly. The local magnetic moment of the scandium doped gold system is quenched because of the strong pairing effect between the scandium 3*d* electrons and gold 6*s* electrons. This is similar to the pairing effect between the 4*s* electrons of Cu atom and the 2*s*, 2*p* electrons of NCO species in Cu_nNCO clusters of our work.

Comparison of Results with other Works

In order to compare the findings of this study with those of the others, we list some calculated results for Cu_nNCO (n = 1-6) clusters obtained from ref [19] in Table 5. Similar characteristics, such as N-C bond-length contraction, C-O bond-length elongation and the odd-even oscillation of adsorption energies are clearly noticeable, while some discrepancies can also be easily found. The N-C bond-length contraction ratio, C-O bond-length elongation ratio, adsorption

Table 4. The Calculated Highest Vibrational Frequencies of Cu-Cu, Cu-N and N-C-O Mode for Cu_nNCO Clusters, Pure Cu_n Clusters and NCO Species

Cluster	ν_{Cu-Cu} (cm^{-1})	ν_{Cu-N} (cm^{-1})	ν_{N-C-O} (cm^{-1})	Cluster	ν_{Cu-Cu} (cm^{-1})	ν_{Cu-N} (cm^{-1})	ν_{N-C-O} (cm^{-1})
NCO			1993.3	Cu_8NCO	251.3	554.1	2260.5
CuNCO		636.5	2157.9	Cu_8	270.9		
Cu_2NCO	237.5	579.7	2190.2	Cu_9NCO	267.6	587.7	2256.3
Cu_2	273.2			Cu_9	258.9		
Cu_3NCO	258.1	586.0	2271.0	$Cu_{10}NCO$	227.2	567.1	2243.7
Cu_3	257.7			Cu_{10}	251.0		
Cu_4NCO	260.5	564.0	2264.5	$Cu_{11}NCO$	301.3	588.8	2252.9
Cu_4	269.5			Cu_{11}	295.5		
Cu_5NCO	279.5	574.8	2271.2	$Cu_{12}NCO$	289.0	575.6	2246.3
Cu_5	278.1			Cu_{12}	275.1		
Cu_6NCO	282.0	556.9	2266.5	$Cu_{13}NCO$	283.6	586.5	2259.7
Cu_6	280.9			Cu_{13}	279.9		
Cu_7NCO	246.0	569.5	2273.9				
Cu_7	251.3						

Table 5. Some Calculated Results for Cu_nNCO (n = 1-6) Clusters Obtained from Ref. [19]

Cluster	$\Delta R_{N-C}/R_{N-C}$ percentage	$\Delta R_{C-O}/R_{C-O}$ percentage	E_{ad} (eV)	Charge				ν_{N-C-O} (cm^{-1})
				NCO	N	C	O	
CuNCO	1.717%	0.509%	3.260	-0.81	-0.99	0.75	-0.57	2195.1
Cu_2NCO	1.226%	0.000%	2.450	-0.90	-1.16	0.80	-0.54	2191.2
Cu_3NCO	1.308%	0.170%	4.050	-0.89	-1.13	0.79	-0.55	2184.3
Cu_4NCO	1.390%	0.000%	3.450	-0.86	-1.12	0.79	-0.54	2196.9
Cu_5NCO	1.308%	0.000%	4.250	-0.85	-1.11	0.80	-0.54	2199.3
Cu_6NCO	1.308%	0.085%	3.400	-0.85	-1.11	0.80	-0.54	2198.6

energy, charge transfer from Cu_n to NCO species and the highest vibrational frequency of N-C-O mode are obviously larger than those of similar studies (see Tables 2, 3, 4 and 5). These discrepancies may be explained in terms of the scalar relativistic effect. The scalar relativistic effect promotes the charge transfer between frontier molecular orbitals of Cu_n cluster and NCO species, thus strengthens the Cu-NCO bonding and gives more prominence to the 2π molecular orbitals in NCO characterized by the bonding orbital between N and C and the anti-bonding orbital between C and O, appearing as the enhancement of N-C bond-length shortening and C-O bond-length lengthening.

CONCLUSIONS

In this paper, an all-electron scalar relativistic calculation on Cu_nNCO (n = 1-13) clusters has been made by using density functional theory with the generalized gradient approximation at the BLYP level. The main conclusions are summarized as follows:

(1) For all Cu_nNCO (n = 1-13) clusters, the NCO species prefered to occupy the single-fold coordination site. The small copper clusters tended to bond with nitric. The Cu_n structures were only distorted slightly and the NCO species retained linear structure without bent. The N-C bond-length contraction and C-O bond-length elongation were observed. The reactivity enhancement of NCO species toward CO_2 was obvious. Unfortunately, no reactivity enhancement of NCO to form N_2 related to the N-C bond strength could be found.

(2) The highly favorable adsorption between small copper cluster and NCO species took place when NCO was adsorbed onto an odd-numbered pure Cu_n cluster and became odd-numbered Cu_nNCO cluster with even number of valence electrons.

(3) The odd-even alteration of magnetic moments was observed in Cu_nNCO clusters which could serve as the material with tunable code capacity of “0” and “1” by adsorbing NCO species onto odd or even-numbered small copper cluster.

(4) The N-C bond-length contraction ratio, C-O bond-length elongation ratio, adsorption energy, charge transfer from Cu_n to NCO species and the highest vibrational frequency of N-C-O mode in our work were obviously larger than those of others. These discrepancies may be explained in terms of the scalar relativistic effect.

ACKNOWLEDGEMENTS

This work was supported by the Nature Science Foundation of Chongqing city, China. No. CSTC-2007BB4137.

REFERENCES

[1] R.M. Heck, R.J. Farrauto, Catalytic Air Pollution Control, Commercial Technology, International Thomson Publishing, New York, 1995

[2] R.A. Perry, D.L. Siebers, Nature 324 (1986) 657.

[3] J.A. Miller, C.T. Bowman, Int. J. Chem. Kinet. 23 (1991) 289.

[4] Z.G. Wei, X.R. Huang, Y.B. Sun, S.W. Zhang, C.C. Sun, J. Mol. Struc. THEOCHEM 679 (2004) 101.

[5] A.R. Balkenende, G.J.G. van der Grift, E.A. Meulenkamp, J.W. Geus, Appl. Surf. Sci. 68 (1993) 161.

[6] H. Permana, K.Y. Simon Ng, C.H.F. Peden, S.J. Schmieg, D.K. Lambert, D.N. Belton, J. Catal. 164 (1996) 194.

[7] V.P. Zhdanov, B. Kasemo, Surf. Sci. Rep. 29 (1997) 31.

[8] A. Prestianni, A. Martorana, F. Labat, I. Ciofini, C. Adamo, J. Mol. Struc. THEOCHEM 903 (2009) 34.

[9] N.S. Phala, G. Klatt, E.V. Steen, Chem. Phys. Lett. 395 (2004) 33.

[10] X.L. Ding, J.L. Yang, J.G. Hou, Q.S. Zhu, J. Mol. Struc. THEOCHEM 755 (2005) 9.

[11] M. Okumura, Y. Kitagawa, M. Haruta, K. Yamaguchi, Appl. Catal. A 291 (2005) 37.

[12] S. Chretien, M.S. Gordon, H. Metiu, J. Chem. Phys. 121 (2004) 9931.

[13] Y. Wang, X.G. Gong, J. Chem. Phys. 125 (2006) 124703.

[14] G. Mills, M.S. Gordon, H. Metiu, Chem. Phys. Lett. 359 (2002) 493.

[15] S. Zhao, Z.H. Li, W.N. Wang, K.N. Fan, J. Chem. Phys. 122 (2005) 144701.

[16] L. Padilla-Campos, J. Mol. Struc. THEOCHEM 851 (2008) 15.

[17] L. Padilla-Campos, J. Mol. Struc. THEOCHEM 815 (2007) 63.

[18] X.H. Cheng, M.X. Jin, Z. Hu, D.J. Ding, Chin. J. Chem. Phys. 21 (2008) 445.

[19] S. Zhao, Y.L. Ren, J.J. Wang, W.P. Yin, J. Phys. Chem. A 113 (2009) 1075.

[20] J.M. Hu, Y. Li, J.Q. Li, Y.F. Zhang, W. Lin, G.X. Jia, J. Solid. State. Chem. 177 (2004) 2763.

[21] N.J. Castellani, R.M. Ferullo, J. Mol. Catal. A 221 (2004) 155.

[22] G.R. Garda, R.M. Ferullo, N.J. Castellani, Surf. Sci. 598 (2005) 57.

[23] R.M. Ferullo, G.R. Garda, P.G. Belelli, M.M. Branda, N.J. Castellani, J. Mol. Struc. THEOCHEM 769 (2006) 217.

[24] S. Zhao, Y.L. Ren, J.J. Wang, W.P. Yin, J. Mol. Struct. THEOCHEM 897 (2009) 100.

[25] E.M. Fernandez, J.M. Soler, L.L. Garzon, C. Balbas,

Phys. Rev. B 70 (2004) 165403.
[26] J. Autschbach, S. Siekierski, M. Seth, P. Schwerdtfeger, W.H.E. Schwarz, J. Compu. Chem. 23 (2002) 804.
[27] H. Orita, N. Itoh, Y. Inada, Chem. Phys. Lett. 384 (2004) 271.
[28] Y.S. Lee, A.D. McLean, J. Chem. Phys. 76 (1982) 735.
[29] S.N. Datta, C.S. Ewig, Chem. Phys. Lett. 85 (1982) 443.
[30] B. Delley, J. Chem. Phys. 92 (1990) 508.
[31] B. Delley, J. Chem. Phys. 113 (2000) 7756.
[32] V.A. Spasov, T.H. Lee, J. Chem. Phys. 99 (1993) 6308.
[33] C.Y. Cha, G. Gantefor, J. Chem. Phys. 112 (2000) 1713.
[34] V.B. Kouteck, J. Gaus, M.F. Guest, L. Cespiva, J. Kouteck, Chem. Phys. Lett. 206 (1993) 528.
[35] H. Celio, K. Mudalige, P. Mills, M. Trenary, Surf. Sci. 394 (1997) L168.
[36] P. Calaminici, A.M. Koster, N. Russo, D.R. Salahub, J. Chem. Phys. 105 (1996) 21.
[37] D. Danovich, S. Shaik, J. Chem. Theory Comput. 6 (2010) 1479.
[38] P.B. Balbuena, P.A. Derosa, J.M. Seminario, J. Phys. Chem. B 103 (1999) 2830.
[39] Q. Zeng, X. Wang, M.L. Yang, H.B. Fu, Eur. Phys. J. D 58 (2010) 125.
[40] A. Chaudhari, S.H. Lee, Int. J. Quant. Chem. 107 (2007) 212.
[41] F. Solymosi, T. Bansagi, J. Catal. 156 (1995) 75.
[42] F. Boccuzzi, S. Coluccia, G. Martra, N. Ravasio, J. Catal. 184 (1999) 316.
[43] P. Misra, C.W. Mathews, D. Ramsay, A.J. Mol. Spectrosc. 130 (1988) 419.
[44] R.A. Copeland, D.R. Crosley, Can. J. Phys. 62 (1984) 1488.
[45] K.N. Wong, W.R. Anderson, A.J. Kotlar, J. Chem. Phys. 81 (1984) 2970.
[46] X.L. Ding, Z.Y. Li, J.L. Yang, J.G. Hou, Q.S. Zhu, J. Chem. Phys. 121 (2004) 2558.
[47] M.E. Eberhart, R.C. Handley, K.H. Johnson, Phys. Rev. B 29 (1984) 1097.
[48] J.L. Yang, F. Toigo, K.L. Wang, Phys. Rev. B 50 (1994) 7915.
[49] M. Zhang, L.M. He, L.X. Zhao, X.J. Feng, W. Cao, Y.H. Luo, J. Mol. Struct. THEOCHEM 911 (2009) 65.
[50] M.B. Torres, E.M. Fernández, L.C. Balbás, Phys. Rev. B71 (2006) 155412.
[51] C. Majumder, A.K. Kandalam, P. Jena, Phys. Rev. B74 (2006) 205437.
[52] E. Janssens, H. Tanaka, S. Neukermans, R.E. Silverans, P. Lievens, Phys. Rev. B69 (2004) 085402.